Published in final edited form as:
J Control Release. 2012 July 20; 161(2): 338–350. doi:10.1016/j.jconrel.2012.01.018.

Locoregional Drug Delivery Using Image-guided Intra-arterial Drug Eluting Bead Therapy

Andrew L. Lewis[1,*] and **Matthew R. Dreher**[2]

[1]Biocompatibles UK Ltd, Farnham Business Park, Weydon Lane, Farnham, Surrey, GU9 8QL, UK

[2]Center for Interventional Oncology, Radiology and Imaging Sciences, Clinical Center & National Cancer Institute, National Institutes of Health, Bethesda, MD, USA

Abstract

Lipiodol-based transarterial chemoembolization (TACE) has been performed for over 3 decades for the treatment of solid tumors and describes the infusion of chemotherapeutic agents followed by embolization with particles. TACE is an effective treatment for inoperable hepatic tumors, especially hypervascular tumors such as hepatocellular carcinoma. Recently, drug eluting beads (DEBs), in which a uniform embolic material is loaded with a drug and delivered in a single image-guided step, have been developed to reduce the variability in a TACE procedure. DEB-TACE results in localization of drug to targeted tumors while minimizing systemic exposure to chemotherapeutics. Once localized in the tissue, drug is eluted from the DEB in a controlled manner and penetrates hundreds of microns of tissue from the DEB surface. Necrosis is evident surrounding a DEB in tissue days to months after therapy; however, the contribution of drug and ischemia is currently unknown. Future advances in DEB technology may include image-ability, DEB size tailored to tumor anatomy and drug combinations.

Keywords

Transarterial chemoembolization; drug eluting bead; hepatocellular carcinoma; drug delivery; drug penetration; pharmacokinetics

1.0 Introduction

Ehrlich's concept of a "Magic Bullet" [1] has inspired generations of scientists in their pursuit of drug therapies with improved efficacy and reduced side effects; by more specific delivery to the target site (at the organ, cell and sub-cellular level). This Holy Grail has become somewhat of an obsession for the drug delivery community, and when combined

*Corresponding author, Tel: +44 (0)1252 732 819, Fax: +44 (0)1252 732 777, andrew.lewis@biocompatibles.com.

Figures 6 and 9 reprinted from Journal of Hepatology, 55(6), Namur et al, Embolization of hepatocellular carcinoma with drug-eluting beads: doxorubicin tissue concentration and distribution in patient liver explants, 1332–8, 2011, with permission from Elsevier. Figures 7, 8 and 11 reprinted from Journal of Vascular and Interventional Radiology, Dreher et al, Radiopaque Drug-Eluting Beads for Transcatheter Embolotherapy: Experimental Study of Drug Penetration and Coverage in Swine, doi:10.1016/j.jvir.2011.10.019, with permission from Elsevier. Figure 10 reprinted from Journal of Vascular and Interventional Radiology, 21(6), Sharma et al, Development of "imageable" beads for transcatheter embolotherapy, 865–76, 2010, with permission from Elsevier.

with the emergence of nanotechnology, has given rise to a vast array of nano drug delivery systems (DDS) [2]. Common DDS include liposomes [3], micelles [4], and macromolecular drug carriers [5, 6]. These approaches often use ligands to recognize specific cell surface motifs [7]. The foundation of nano DDS is based on the enhanced permeability and retention (EPR) effect for tumor accumulation [8, 9]. The EPR effect describes the passive accumulation of long circulating DDS in a solid tumor which is due to the greater vascular permeability and lack of functional lymphatics [10–12]. Despite the advances and promises nano DDS have demonstrated *in vitro* and pre-clinically, relatively few have translated into commercially-successful therapies with proven clinical benefits [8, 13].

Even though device-based DDS (such as Gliadel® and Lupron Depot®) have proven clinical success [14], they have recently received less attention in the wave of nanomedicine especially for cancer therapy. Microparticle-based DDS (20μm-1000μm) are relatively simple to manufacture out of biocompatible materials. These DDS are capable of holding large quantities of drugs and delivering these drugs in a controlled manner, often well described by an elution profile. The administration of device-based DDS to a patient is not as simple or elegant as nano DDS, often requiring surgery or other invasive means. Alternative administration routes such as the use of intra-arterial infusion has a rich history of effective clinical practice in cancer therapy for both chemotherapy and radiotherapy (i.e., radioembolisation), especially for primary and secondary hepatic malignancies [15–17]. Hepatic arterial infusion of chemotherapy may be very effective when the drug is properly chosen to be fully extracted by the tissue of interest [18–20] and tumor feeding arteries may be selected with a catheter by a physician, typically an interventional radiologist. This review will focus on the use of microparticle-based DDS for the intra-arterial therapy of solid tumors.

1.1 Basics of transarterial chemoembolization

Transartererial chemoembolization (TACE) has been practiced in patients for over 3 decades [21, 22] and describes the infusion of chemotherapeutic agents followed by embolic particles [23]. Although there is no worldwide standard technique, chemotherapeutics may be emulsified with Lipiodol® which is a radiopaque contrast agent composed of iodinated ethyl esters of fatty acids from poppyseed oil (37wt% Iodine). This infusion is normally performed by selecting tumor feeding arteries with a catheter under image guidance (see Figure 1) [17, 24]. TACE for hepatic malignancies is successful because these tumors have predominant arterial blood supply while the remaining normal liver perfusion consists mostly of portal blood flow. This arterial preference may provide some degree of selectivity to the tumor while limiting ischemic and/or cytotoxic injury to the normal liver parenchyma due to patent portal blood flow following TACE. The overall goal of TACE is to deliver a high dose of drug directly to a tumor, prevent drug clearance, and induce ischemic necrosis of the tumor [17]. Interestingly, some of the initial work by Maeda et al that led to defining the EPR effect used an intra-arterial delivery route with Lipiodol [25].

1.2 Overview of drug eluting beads in transarterial chemoembolization

Despite the widespread use of TACE, there remains tremendous variability in material choice and procedural technique, with a lack of clear consensus or standardization [23, 24, 26–28]. For example, there is variability in: 1) type and size of embolic agent, 2) type and amount of chemotherapeutic agent(s), 3) degree of catheter selectivity (i.e., a measure of how distal the catheter tip is positioned in an arterial network), and 4) optimal embolization endpoint (i.e., the reduction in antegrade flow when the procedure is concluded) [29–32]. Recently, drug-eluting beads (DEBs), in which a uniform embolic material is loaded with a drug and delivered in a single image-guided step, have been used more frequently in the clinic. This approach is in contrast to “conventional” lipiodol-based TACE where

chemotherapeutics and embolic agents are often delivered sequentially. DEBs have potential to simplify and standardize the TACE procedure by first preloading the embolic with drug followed by controlled drug elution once localized in the target tissue [33–38]. This DEB-TACE approach also provides simultaneous delivery of the embolic and drug in the target tissue, ensuring that clearance is minimized when the drug is present.

The DEB is not a new concept. As early as 1983 an excellent review was published by Tomlinson that highlights some of the important considerations for microsphere drug delivery including loading, elution, physicochemical properties, and delivery [39]. This was further expanded upon in a review of microparticulate drug delivery systems for embolization by Kerr in 1987 [40]. Over around a twenty year period following these reviews, a large number of reports can be found in the literature covering *in vitro*, pre-clinical and even clinical studies utilizing drug-loaded microspheres for chemoembolization, some of which are summarized in a book chapter by Lewis [41]. These studies used microspheres composed of either non-degradable and degradable systems based on synthetic polymers such as poly(lactic/glycolic acid), poly(hydroxybutyrate), ethylene vinyl acetate, or natural materials such as albumin, gelatin, chitosan or aliginate; with microsphere sizes falling roughly into two categories- 15–60 μm and 100–250 μm. Drugs of choice included doxorubicin, mitomycin C, cisplatin, methotrexate and paclitaxel amongst many others, with a drug loading range of 1–65wt% [41]. Clearly, given the variability of embolization technique, microsphere materials and drug identity between studies, there was little evidence generated to indicate improved efficacy of one system over another.

The use of DEB in TACE was reinvigorated in 2007 by two clinical reports demonstrating safety and efficacy (i.e. clinical response) [42, 43]. One of the most common DEB in clinical use today is DC Bead® (DC Bead, Biocompatibles UK Ltd, known as LC Bead® in the USA) [37, 44], which is the primary focus of this review as more published data is available. Since 2005, there have been over 70,000 clinical treatments worldwide with DC Bead. DEB-TACE using DC Bead is most commonly performed with Doxorubicin (known as DEBDOX™) or Irinotecan (known as DEBIRI™). HepaSphere® (Merit Medical, known as QuadraSphere® in the USA) is another commercially available DEB in clinical use [45–50]. Additional studies are warranted to investigate the difference between these two DEB technologies.

1.3 Clinical evidence for TACE and DEB-TACE

TACE has been practiced around the world for many years largely driven by each physician's experience, using techniques that vary considerably from one hospital to the next. Sporadic reports supported the benefit of TACE but it was not until 2002 that two independently conducted randomized controlled trials demonstrated a statistically significant survival benefit for conventional Lipiodol-based TACE *versus* best supportive care [51, 52]. Later, with the introduction of DEB into the clinic, two phase I/II studies to determine safety and the pharmacokinetic profile for DEB-TACE were performed [42, 43]. Importantly, DEB-TACE significantly reduced the peak plasma drug concentration and area under the curve *versus* conventional Lipiodol-based TACE or hepatic arterial infusion (see Figure 2), as evidenced by both pre-clinical (Figure 2B) [53] and these human clinical studies (Figure 2A) [42, 43]. These data suggest that the reduced systemic toxicity observed in DEB-TACE may be due to the limited systemic exposure of this locoregional therapy.

1.3.1 DEB-TACE *versus* bland embolization and conventional Lipiodol-based TACE—A randomized clinical trial in 212 patients with HCC demonstrated that DEB-TACE is better tolerated than conventional Lipiodol-based TACE, and that DEB-TACE was more effective in patients with more advanced disease (defined as Child-Pugh B, ECOG 1,

bilobar disease, and recurrent disease) [54]. Although this trial failed to reach statistical significance, there was a trend in the DEB-TACE group towards better complete response, objective response, and disease control compared to conventional TACE [54]. A retrospective study demonstrated that DEB-TACE provided a survival benefit over treatment with conventional TACE in patients with unresectable HCC [55]. Although the theory of TACE was built around the concept of trapping chemotherapy in the tumor and reducing its washout, a pharmacokinetic study performed by Johnson *et al* demonstrated that when doxorubicin was emulsified with Lipiodol without an additional embolic, levels in the systemic circulation were similar post Lipiodol-based TACE to those from simple intra-arterial hepatic administration of doxorubicin [56]. Recently in a preclinical Vx2 model, it was demonstrated that Lipiodol deposition in a tumor (measured by CT attenuation) did not correlate with the amount of doxorubicin delivered to the tumor [57]. These data suggesting that Lipiodol rapidly releases doxorubicin consistent with in vitro elution assays [37].

A prospective randomized controlled trial also showed that DEB-TACE provided a better local response, fewer recurrences, and a longer time to progression when compared with bland beads of the same size, although no statistical difference in overall survival was observed [58]. In principal, both bland embolization and DEB-TACE should be effective due to the induced ischemia resulting in an initial response, but it is possible that the drug provides an added benefit of limiting recurrence or time to progression. In the setting of metastases to the liver, the drug may be beneficial to treat micro-metastatic liver disease not apparent on conventional imaging due to selective activity of chemotherapeutics to cancer cells.

1.3.2 DEB-TACE in HCC—There have been a number of studies that have reported on the use of DEBDOX to treat HCC, most of which use response rates as a measure of therapeutic efficacy (usually by either EASL [European Association for the Study of the Liver] or RECIST [Response Evaluation Criteria in Solid Tumors] criteria). A recent review of the literature [24] reported on 8 published DEB-TACE studies in a total of 353 HCC patients and found complete or partial responses at 6 months in the range 44–80.6% (by EASL criteria). Long-term follow-up is still on-going in some studies but there are very promising 2 year survival rates in the range of 55–91.1 %. A randomized Phase II study (PRECISION V) reported objective response rate of 52% for DEBDOX *vs* 44% for Lipiodol-based TACE (by EASL), which although not statistically significant across the entire patient population, revealed a significant advantage of DEBDOX for patients with advanced liver disease [54]. DEBDOX is therefore proving to be an effective treatment for HCC, with its use expanding into other treatment regimes, such as for patients prior to orthotopic liver transplant [59] or in earlier stage patients in combination with RFA [60, 61].

1.3.3 DEB-TACE in metastatic colorectal carcinoma (mCRC) to the liver—The use of DEB-TACE to treat mCRC is still in its infancy but growing rapidly [62–64]. The approach of the technique is fundamentally different for metastatic disease where tumors may be more diffuse and less vascular than HCC. Irinotecan is the favored drug due to its activity in colorectal cancer and DEBIRI has been performed as a monotherapy in 3rd line patients or in combination with systemic therapies in first and second line settings. A more lobar infusion of smaller sized beads (70–150 or 100–300 μm) of up to 200 mg irinotecan is preferred over the more super-selective approach to HCC. This lobar infusion is used because mCRC often presents as more diffuse disease throughout the liver rather than then a solitary focal lesion that are often found with HCC. Early clinical data are very encouraging, with local disease control rates of >60% (by modified RECIST criteria) [62–64] with one study reporting a statistically significant improvement in median overall survival compared to chemotherapy (FOLFIRI) of 23 *versus* 15 months [65]. Some patients treated with

DEBIRI have been subsequently down-staged to surgery, which demonstrates the feasibility of this treatment in a neoadjuvant setting [66].

1.3.4 DEB-TACE in other malignancies—As DEB-TACE becomes more established in the treatment of HCC and the early positive results emerge from its use in mCRC therapy, the approach is also being investigated as a potential therapy in the treatment of a variety of other liver tumor histologies. It is feasible to treat patients suffering with low-grade gastroenteropancreatic endocrine tumors, which have metastasized to the liver with DEBDOX, resulting in response rates of 80% [67]. DEBDOX has also been used in patients with intrahepatic cholangiocarcinoma, with a response rate of 100% at 3 months [62]. Others have chosen to treat these patients with DEBIRI (sometimes in combination with systemic therapies) and have demonstrated improved median overall survival for the combined DEB + systemic regimen compared to chemotherapy alone (17.5 *vs.* 7.4 months, P=0.02) [68]. In a study of 10 patients with uveal melanoma metastases to the liver treated with DEBIRI at a dose of 100mg, all had an objective response, three with a very good partial response and encouraging survival data given this particularly devastating disease [69]. Clearly both DEBDOX and DEBIRI have a part to play in the treatment of hepatic cancers beyond HCC and mCRC.

2. Principles of DEB

2.1. Chemistry

A wide range of synthetic and natural biodegradable polymeric microspheres ranging in sizes between 10–400 μm, have been described as vehicles for the delivery of a similarly broad variety of chemotherapeutic agents *via* intra-arterial administration [41]. Whilst many of these systems demonstrated some potential efficacy, the development of a commercially-viable product was hampered by an inability to iterate and therefore optimize the therapy by selection of appropriate drug, dose, release kinetics (e.g. degradation rate) and delivery vehicle size. The advent of compressible embolization microspheres available in a series of calibrated diameters (often defined by a diameter size range) provided an interventional radiologist with a device that could be delivered through a microcatheter for more reproducible targeting of tissue lesions [70, 71]. A major advancement was made in 2004 when calibrated microspheres were synthesized that were able to load charged chemotherapeutic agents by virtue of the inclusion of ionic binding moieties within the microsphere structure [37]. These so-called drug-capable beads (hence DC Bead) offered the option for a physician to load a choice of appropriate anticancer drugs, in therapeutically meaningful doses, into an embolization device with a range of sizes. This has enabled some degree of standardization of the TACE procedure and potential to identify the most efficacious combination of drug, dose, size and technique.

The capability to load positively-charged drugs is a consequence of the inclusion of anionically-charged functional groups pendent to the polymer chains. The microspheres are formed from a high water content hydrogel based upon polyvinyl alcohol (PVA), a biocompatible non-biodegraded polymer with proven use in biomedical applications and as an embolic microparticulate for several decades [72]. The PVA is chemically modified to create a macromonomer capable of participating in free radical polymerization with acrylic monomers. An inverse suspension polymerization is used to prepare microspheres of the PVA-acrylic hydrogel hybrid. By appropriate selection of the acrylic comonomer, various functionality can be introduced into the polymer network; 2-acrylamido-2-methylpropane sulfonate (AMPS) was chosen for its potential biocompatibility, thermal stability and the presence of charged sulfonate groups (Figure 3A).

The subsequent hydrogel beads have a high water content (>95%) which enables diffusion of water-soluble small molecules into the network structure. When the molecule is a positively charged drug, it may interact reversibly with the sulfonate groups by ion-exchange to displace the sodium counter ion from the AMPS and secure the drug into the structure by ionic interactions. Evidence for this interaction is provided by Fourier Transform infra-red spectroscopy, which clearly demonstrated an increasing shift to lower wavenumber of the sulfonate S=O stretch with increasing amount of drug bound, as shown in Figure 3B and C**Error! Reference source not found.**. This technique can also be used to image and map the drug distribution across thin sections of the beads and moreover, that remaining in beads and tissue using histological slides [73, 74].

2.2. Drug loading and elution

The rate of uptake of a particular drug increased with decreasing size of the beads due to the relative increase in surface area to volume ratio. As can be seen from Figure 4, when drug is sequestered into the bead structure, it may change color if the drug itself is colored (as for doxorubicin which is red (Figure 4b&e), mitoxantrone which is an intense blue (Figure 4c), or irinotecan which is straw yellow, yielding a turquoise color when loaded into the blue beads (Figure 4f)). Moreover, as the drug interacts with the bead structure, water is displaced from the hydrogel, lowering the water content, increasing the compressive modulus and resulting in a decrease of the average bead diameter [36, 38]. Note in Figure 4 that mitoxantrone (Figure 4c) has two cationic binding groups compared to one for doxorubicin (Figure 4b) and hence interaction is stronger, resulting in a greater decrease in diameter. Both of these drugs are anthracene dione derivatives which are conducive for stacking *via* pi-pi interactions between the fused aromatic ring systems. These drug-drug interactions can be the over-riding influence on how tightly the drug will bind within the bead and hence dictate their overall rate of release.

The subsequent elution profile of a drug may therefore be described as a function of not only the ionic strength and composition of the elution medium but also dependent upon the nature and degree of drug-polymer and drug-drug interactions. Again, the size of the beads is an important determinant of elution rate, as the surface area to volume ratio comes into play. The rate of release can be determined *in vitro* by a variety of different elution methods; the simplest being a USP II apparatus in which all of the drug can be eluted rapidly by selection of an appropriate elution medium under sink conditions (Figure 5). This technique, whilst useful from a product development and quality control perspective, offers no insight into how rapidly the drug might be released in vivo. Various other apparatus such as the USP IV flow-through cell or T-apparatus have been described, which have been shown by *in vitro in vivo* correlation to better predict the fraction of drug that is released into the systemic circulation following DEB administration [34, 46].

The dose used for DEBDOX is typically 25–37.5 mg doxorubicin/mL of beads, with 2–4 mL of beads generally administered in the treatment of HCC making the total dose in the range 50–150 mg doxorubicin. For DEBIRI, a loading of 50 mg of irinotecan/mL beads is recommended, with up to 4mL (200 mg total irinotecan) administered per treatment (typically for metastatic colorectal cancer to the liver with a lobar infusion), although less drug than this is commonly used but then on a more frequent repeat schedule.

HepaSphere is composed of a polyvinyl alcohol – acrylic acid superabsorbent copolymer that can swell up to 64x its initial volume. It interacts with drugs by much the same mechanism as DC Bead, only *via* ionic interactions with the carboxylate groups instead of sulfonate groups. This gives rise to similar elution characteristics when doxorubicin is used as the drug-drug interactions predominate coulombic forces, whereas interaction between the carboxylate and irinotecan is particularly weak and hence elution is more rapid [46].

3. Locoregional drug delivery

Locoregional drug delivery may be clinically warranted when a cancer patient has unresectable disease. Often systemic therapy may be ineffective or not well tolerated by these patients. It is important to note that although locoregional drug delivery may be effective at a local targeted site, there is little evidence that such local therapies may influence widespread systemic disease. In this regard, it is becoming more common for systemic therapies, such as sorafenib, sunitinib or everolimus, to be combined with DEB-TACE; this is currently being evaluated in clinical trials [76]. We will focus our discussion on liver directed locoregional drug delivery with DEB-TACE. Additional trancatheter intra-arterial therapies, including embolization, intra-arterial infusion, TACE, DEB-TACE and radioembolization was recently reviewed [17].

Locoregional drug delivery may be examined at many length scales: whole body, organ/tissue, tumor and cellular. Figure 2 suggests that most of the delivered dose in DEB-TACE with doxorubicin is confined to the liver, because the peak plasma drug concentration and AUC are dramatically reduced with DEB-TACE compared to conventional Lipiodol-based TACE or intra-arterial infusion. This reduced systemic exposure on whole body scale implies that DEB-TACE is effective at localizing the drug to the desired organ/tissue. In one perspective, DEB-TACE may be considered the most extreme EPR effect in that the commonly used drugs (Doxorubicin and Irinotecan) are sufficiently permeable due to their physicochemical properties (e.g., low MW) and retention is high since the predominant clearance route, the blood vessels, are eliminated. However, confining a drug to the desired organ does not imply that the drug is entirely bioavailable (contained by the bead or free) in the desired region or targeted cellular population. The following sections will examine the known data on DEB-TACE and drug location at various length scales as well as the tissue effects.

3.1. Bead penetration into the tumor

After DEB is infused through a catheter into an artery directed at a tumor, the intension or belief is that the DEB will be carried by blood flow directly to the tumor. Preferential arterial supply of the tumor should help tumor selectivity but the final location of the DEB will depend on the physical interaction of the bead (e.g., size, mechanical and surface properties) with the tissue (e.g., architecture of the arterial system and blood flow). Geschwind and colleagues demonstrated in a preclinical Vx2 tumor model that DEB-TACE provides greater tumor concentration of drug (max = 413.5 nmol/g, at 3 days) than traditional Lipiodol-based TACE (12–36 nmol/g) [53]. Although the exact location of the DEB and drug in a tumor or drug bioavailability was unknown, these data motivated the use of DEB-TACE to provide improved tumor exposure.

Laurent and colleagues recently provided valuable clinical evidence, although in only one patient, on the DEB location in an explanted liver, as shown in Figure 6 [75]. They demonstrated that most of the beads are confined within 10 mm of the tumor boundary with 58% of the occluded blood vessels in normal liver and 42% of the occluded blood vessels found in the tumor with a mean tumor penetration of 3.8 ± 3.7 mm from the tumor boundary. The mean embolized blood vessel size was 237±135 μm, very comparable to the size of DEBs used in this patient (100–300μm DC Bead). Although limited data exist, it is rational that most of the DEBs may be routinely found in the tumor periphery and surrounding normal tissue due to the size of the DEBs and the enlarged tumor blood vessels and greater vascularity often found at the tumor margin [75].

3.2. Drug distribution surrounding DEBs

Once the DEB is delivered to the target tissue, the drug may be eluted into the surrounding tissue. The spatial distribution of the drug will depend on the drug elution profile as well as the interaction between the drug and the tissue. The fluorescent properties of doxorubicin were used to visualize doxorubicin distribution with fluorescence microscopy [77]. Initially, substantial quantities of drug were contained within the DEB but this diminished dramatically over 24 hours. Doxorubicin levels within the tissue were greatest immediately surrounding the DEB and declined over hundreds of microns from the bead surface. Semi-quantitative image analysis was used to document the penetration of doxorubicin from the bead surface over 1 week following DEB-TACE as shown in Figure 7. Thirty minutes following embolization, the drug levels were very high (~30–40 μM) adjacent to the DEB surface. The overall concentration increased from 30 min to 1 hr, and remained markedly elevated up to 8 hours following embolization. After 24 hr, the concentration substantially declined to ~0.5–5.0 μM for distances up to 150 μm from the DEB surface. One week following embolization, doxorubicin was still detected but the concentration was much lower. Laurent and coworkers have used microspectrofluorimetry, which is a more rigorous and quantitative technique, to measure doxorubicin penetration for time periods up to 90 days [73, 75]. The overall shape of the penetration profile is similar to that presented in Figure 7 suggesting diffusion dominated transport. In resected liver tumors, the mean concentration surrounding the DEBs ranged from 5 μM at 8 hours to 0.65 μM at 32–36days [75].

3.3. Tissue effects

It is important to note that drug localized to the tissue in DEB-TACE is not immediately 100% bioavailable. Much of the drug is initially held by the DEB and is then eluted in a controlled fashion to become bioavailable. Confocal microscopy in **Error! Reference source not found.** demonstrates the intracellular uptake and subcellular distribution of doxorubicin. Doxorubicin was found surrounding normal hepatocytes in swine liver 30 min after embolization followed by strong nuclear localization by 1 hr that increased up to 8 hr. Cellular organization and tissue architecture were affected by 24hr with less cellularity observed by 7 days.

Explanted liver specimens 9–36 days following DEB-TACE often demonstrated inflammatory-fibrotic tissue as well as coagulative necrosis surrounding the DEBs as shown in Figure 9. At early timepoints between 9 and 14 days, viable liver parenchyma (8% of DEBs) and viable tumor (2% of DEBs) was identified. In other patients at 32–36 days following DEB-TACE, viable tissue disappeared with necrosis observed surrounding 40% of the DEBs and inflammatory-fibrotic tissue was evident around 60% of the DEBs. The localization of necrosis and inflammatory fibrosis to the bead proximity suggests an influence of drug on tissue necrosis but ischemia may also play a significant role.

4. Future directions in DEB-TACE

Although DEB-TACE treatment produced response rates of 44–80.6% in HCC [24] we must ask how, why and where tumors escape this form of therapy? Escape may be broadly classified into two categories: incomplete treatment or ineffective treatment. Incomplete treatment may be due to selecting only a fraction of the tumor feeding arteries to be embolized, thus leaving substantial blood flow to a portion of the tumor. In addition, insufficient quantities of the embolic and/or drug may be delivered to a tumor due to physical properties of a DEB such as unwanted aggregation or too large of a diameter to access the entire tumor, leaving regions under-dosed. The treatment may be ineffective due

to tumor cell resistance to drug and/or ischemia. The following sections will describe advances that may be pursued in the near future to hypothetically improve patient outcomes.

4.1. Image-able DEB-TACE

In contrast to conventional Lipiodol-based TACE, DEB-TACE lacks the intraprocedural imaging feedback of Lipiodol deposition in the target tumor, which is seen with fluoroscopy or CT. During DEB-TACE, the embolization process is monitored by detecting changes in antegrade flow of soluble iodinated contrast in which the DEBs are diluted. The embolization is continued until a desired embolization endpoint is reached or reflux of contrast material into non-target vessels is observed, without specific feedback on DEB or drug location. In order to address this lack of feedback, investigators have developed image-able spherical beads or other particles that can be visualized with magnetic resonance [78–83] and X-ray-based (e.g., fluoroscopy and CT) imaging [84, 85] or both [86]. Image-ability is obtained by trapping the relevant contrast material within the porous particle/bead structure or chemically attaching contrast to the polymer backbone. Knowledge of bead distribution during a procedure may provide useful real-time feedback to modify the intervention and tailor the procedure to a specific patient.

The ability to visualize radiopaque DC bead *in vivo* during and after transcatheter embolization procedures was studied in normal swine liver using clinical fluoroscopy and CT units. Although individual radiopaque beads could not be visualized leaving the catheter tip with real-time fluoroscopy as is observed for iodinated contrast or conventional chemoembolization using Lipiodol, their accumulation in branches of the hepatic and renal arteries was easily visualized with fluoroscopy after approximately 0.4 mL of radiopaque beads and after approximately 0.2 mL with more sensitive CT imaging. Figure 10 depicts the three dimensional spatial distribution of the radiopaque beads shown as a surface shaded display. Radiopaque beads filled the hepatic arterial arborization in a peripheral (furthest from the catheter tip) to central (closest to the catheter tip) fashion demonstrating a dose response. This is different from soluble contrast that opacified the hepatic arteries in a central to peripheral fashion. The discordance between the soluble contrast and the radiopaque bead images emphasized the utility of radiopaque beads as well as the limitations of soluble contrast to indicate bead and/or drug location. The use of radiopaque DEBs in clinical practice may report on embolic location, and since the chemotherapeutics (e.g., doxorubicin and irinotecan) are initially held by the DEB, imaging DEB location may also serve as a surrogate to report on local drug levels, or at least for the location of the drug source.

4.2. Tailor bead size to tumor arterial anatomy

DEB size is one of the key variables that a physician may select. Image-able DEBs may be used as a research tool to investigate the influence of DEB size on eventual tissue localization. Figure 11 shows microCT of swine kidney tissue comparing a more standard size range DEB (100–300 μm) to a smaller size range version (70–150 μm) of the same product. The 70–150 μm DEBs penetrated further into the tissue reaching more distal locations as observed near the renal capsule surface in the axial image of Figure 11. Furthermore, the spatial frequency or density of 70–150 μm DEBs appeared greater than 100–300 μm beads. In normal arterial architecture, smaller arteries or capillaries are more spatially frequent to improve the transport of nutrients to tissues. Tumor blood vessel diameters have reported mean or median values between 12.6 and 55.8 μm but depend on histology and location [87–90]. The improved density of small DEBs in Figure 11 is logical since these smaller DEBs are capable of accessing smaller caliber arteries. The penetration of drug is relatively independent of DEB size [77] suggesting that DEBs with a greater tissue density have potential to yield greater drug coverage. In swine kidney tissue, drug

coverage was increased from 10.9 ± 2.1% to 19.0 ± 3.1% ($P < 0.05$) by decreasing the size range from 100–300 μm to 70–150 μm [77]. The low level of drug coverage (<20%) suggests there is substantial room for improved drug coverage with newer DEB technologies. The initial evidence in the first ~150 patients to be treated with 70–150 μm DEB suggests that greater DEB volume may be delivered, presumably due to an improved access to a greater vascular volume for smaller DEBs.

4.3 Integration with imaging guidance

Although TACE is performed under image guidance, most of the technologies and techniques are borrowed from traditional angiographic procedures. Advancement in TACE-specific imaging techniques may improve the reproducibility and completeness of TACE. X-ray fluoroscopy is used to identify the tumor and monitor changes in tumor blood flow with soluble iodinated contrast, but this assessment is very subjective. Quantitative image processing algorithms may be applied to an angiogram to assess tumor blood flow and the degree of stasis [91]. The emergence of cone beam CT, where a traditional C-arm is used to generate 3D imaging data, may help guide and monitor TACE [92–94]. A combination of cone beam CT and radiopaque DEBs may allow for intraprocedural determination of DEB and/or drug spatial distribution. A DEB-TACE procedure may then be modified in real-time to improve coverage of the entire tumor.

Cone beam CT may also be used to plan and guide a DEB-TACE procedure as shown in Figure 12 [95]. The tumor can be identified and segmented in a semi-automated fashion followed by isolation of tumor feeding arteries. In practice, DEB-TACE planners appear to improve the performance of less experienced physicians and may provide a consistent basis to standardize a treatment [92]. The widespread use of such imaging technologies may help standardize TACE but this would require seamless integration into the clinical workflow to realize the potential clinical impact.

4.4 Degradable drug eluting beads

One question that was raised early in the development of DEB was that of what happens to the beads once all the chemotherapy has been eluted? In those instances where treatment is not complete or the tumor recurs, physicians would like to be able to access a tumor on multiple occasions in order to administer additional DEB-TACE treatments as needed; the current materials are considered non-biodegradable which led to early objections to DEB therapy since it may not be possible to re-enter the feeding artery once this artery had been occluded. However, numerous clinical studies have largely allayed these fears, as it has been generally proven possible to perform multiple repeat DEB-TACE procedures per patient [24]. The potential value of biodegradable DEBs for retreatment has therefore been unfounded, although as with drug eluting stents, there is an undercurrent of opinion that DEB evolution will eventually move in this biodegradable direction as an essential feature. This is likely to be driven by the ability to administer difficult-to-deliver drugs that cannot be delivered *via* existing non-biodegradable DEB technology, rather than by improvement in clinical benefits related to biodegradability.

4.5 DEB Combination Therapies

The current state of cancer therapy involves a combination of various treatments including surgery, chemotherapy and radiation, such as neo-adjuvant chemotherapy prior to surgery. It is likely that DEB-TACE will evolve into part of a comprehensive treatment for certain cancer patients, rather than a stand-alone therapy. Logical combinations in the short term include DEB-TACE and thermal ablative technologies (e.g., radiofrequency ablation, RFA [96]) or concurrent drug combinations (e.g., systemic [97] or delivered on the DEB).

DEB-TACE or Lipiodol-based TACE is well suited for combination with other image-guided locoregional therapies such as RFA [60, 61, 98]. Embolization prior to ablation [61, 98] may reduce tumor perfusion sufficiently to improve size of the ablation by limiting convective heat loss through blood flow [99, 100]. If DEBs were image -able, documenting their distribution following DEB-TACE may serve to guide thermal ablation [101], where the needle can be directed towards tumor tissue with fewer beads and potentially lower drug levels. Alternatively, treatment may be enhanced by performing DEB-TACE following RFA [60].

One argument against the use of embolization to treat tumors is that the incomplete kill of the tumor coupled with hypoxic conditions may lead to the transformation of the cancer cells into a more malignant phenotype that becomes more aggressive in its invasiveness and ultimately more difficult to treat effectively. Indeed, there is evidence that the effect of embolization-induced hypoxia is stabilization of hypoxia-inducible factor – 1α (HIF-1 α) and subsequent up-regulation of pro-survival genes leading to escape from apoptosis, expression of vascular endothelial growth factor (VEGF) and recruitment of a new blood supply [102, 103]. This provides a strong rationale for the combination of DEB-TACE with agents that block pathways of angiogenesis. Several studies are on-going to evaluate the combination of DEB-TACE with oral agents such as sorafenib, sunitinib (both multikinase inhibitors that block VEGF expression by different mechanisms) and everolimus (an inhibitor of mTOR, a cell-signalling protein known to have influence over HIF-1 α regulation) in the treatment of patients with HCC [76]. Similarly, in patients with colorectal metastases to the liver, DEB-TACE is being used to deliver irinotecan locally, in combination with systemic chemotherapy regimens such as FOLFOX and erbitux [76]. It is therefore likely, as with most of the successful cancer chemotherapy regimes, that DEB-TACE will be used as part of a cocktail of anti-cancer agents in order to improve patient outcomes.

Whilst clinical trials aim to understand if there could be complimentary activity from combining DEB-TACE with orally-active new agents, it is conceivable there may still be dose-limiting toxicities that curtail the potential effectiveness of this combination treatment. One possible approach to overcoming this limitation may be to combine two or more drugs within the same or different DEBs and locally deliver the drugs concomitantly to a solid tumor. This may of course, only be a relevant approach where the molecular targets of each of the active agents can be clearly accessed by locoregional administration and their biodistribution and bioavailability within the tissue is in the correct timeframe and at the appropriate tissue concentration in order to bring about synergistic activity. This has been achieved practically, where combinations of doxorubicin or irinotecan with rapamycin (contained within individual or the same DEBs) have been shown to have synergistic effects with *in vitro* cell culture assays [104, 105]. More sophisticated tumor models and techniques are required in order to elucidate which drug combinations and at what relative doses may have such synergistic effects *in vivo*.

4.6 Protein eluting bead

One problem with current DEB technology is that there is a limit to the amount of drug that can be delivered and ultimately the number of times the procedure can be performed. Furthermore, available drugs are largely restricted to small molecules. A unique approach would be to program cells to deliver a peptide or other biomolecule and encapsulate these cells into a bead to be delivered intra-arterially. CellBeads® are composed of immortalized mesenchymal stromal cells that can be engineered to secrete a range of therapeutic proteins, encapsulated in an immune-protective shell of an ultra-pure alginate biopolymer. The resulting beads can be made in dimensions from 150–600 μm in size, containing 60–3000 cells per bead. Once implanted, the CellBeads produce the engineered protein, which can

diffuse across the alginate barrier and into the surrounding tissue [106]. The barrier provides protection against the host's immune response, leading to a prolonged therapeutic delivery period of weeks to months, depending upon the site of implantation. One current application in pre-clinical evaluation is the use of 150 μm CellBeads for intracoronary delivery post myocardial infarction [107]. The intracoronary delivery of an embolic cell bead after myocardial infarction appears counterintuitive at first, but sufficient coronary reserve appeared to exist. Intracoronary delivery has the advantage of securing the all the cells in place, whereas for similar delivery of cells alone the retention is very poor. Recent work suggests the cells remain viable for up to 8 weeks in this xenogeneic setting, which is considered long enough to have a major impact on myocardial salvage and improvement of cardiac function. With a limitless range of therapeutic protein possibilities, the CellBead could be the ultimate DEB of the future.

4.7. Other indications

Many tumors can't be treated with transcatheter approaches due to limitations of vascular access or other contraindications. As DEBs essentially act as controlled-release vehicles, they could be used to treat tumors by direct intratumoral injection. Both doxorubicin and irinotecan eluting beads have been studied for the treatment of brain tumors in two different rat models of glioblastoma. The beads used in these preclinical investigations were DC Bead in the size range 100–300 μm. Whilst both drugs were effective, doxorubicin had a much narrower therapeutic window beyond which toxicity was severe [108–110]. Irinotecan eluting beads have been granted orphan drug status in this indication and are about to undergo first clinical evaluation in patients with recurrent glioblastoma by direct multiple injections of a DEB suspension into the resection cavity of the excised tumor. Other studies have shown that both irinotecan and topotecan eluting beads are active towards PSN1 pancreatic cancer cells [111]. Furthermore, additional studies have shown that it is feasible to administer the beads using endoscopic ultrasound guided needle injection into the pancreas [112]. Finally, doxorubicin and mitoxantrone eluting beads have demonstrated activity in pre-clinical mouse models of peritoneal carcinomatosis from colorectal cancer [113], although the safety of intraperitoneal injections of DEBs would need confirming in appropriate animal models. An interesting regulatory perspective for these non-arterially administered indications is that the DEB are classified and regulated as a drug, whereas for DEB-TACE they are regulated as a device (albeit a drug-device combination product) due to their primary mode of action being a physical occlusion of the blood vessels.

5.0 Conclusion

DEBs represent a relatively simple DDS that are effective in the treatment of hepatic lesions with TACE, especially hypervascular tumors such as HCC. Drug loading and elution, as well as material properties of the DEBs, may be manipulated through rational DDS design. DEB-TACE results in localization of drug to targeted tumors while minimizing systemic exposure to chemotherapeutics. Once localized in the tissue, drug is eluted from the DEB in a controlled manner and penetrates hundreds of microns of tissue from the DEB surface. Necrosis is evident surrounding a DEB in tissue days to months after therapy; however, the contribution of drug and ischemia is currently unknown. Future advances in DEB technology may include image-ability, DEB size tailored to tumor anatomy and drug combinations.

Acknowledgments

This was supported in part by the Center for Interventional Oncology and the Intramural Research Program of the National Institutes of Health (NIH). NIH and Biocompatibles UK Ltd have a Cooperative Research and Development Agreement. The authors would like to thank Drs. Bradford Wood, Karun Sharma Carmen Gacchina

and Elliot levy for their useful discussions. The mention of commercial products, their source, or their use in connection with material reported herein is not to be construed as either an actual or implied endorsement of such products by the National Institutes of Health.

References

1. Ehrlich, P. Collected studies on immunity. 1. John Wiley and Sons; New York: 1906.
2. Allen TM, Cullis PR. Drug delivery systems: entering the mainstream. Science. 2004; 303:1818–1822. [PubMed: 15031496]
3. Torchilin VP. Recent advances with liposomes as pharmaceutical carriers. Nat Rev Drug Discov. 2005; 4:145–160. [PubMed: 15688077]
4. Kataoka K, Harada A, Nagasaki Y. Block copolymer micelles for drug delivery: design, characterization and biological significance. Adv Drug Deliv Rev. 2001; 47:113–131. [PubMed: 11251249]
5. Duncan R. The dawning era of polymer therapeutics. Nat Rev Drug Discov. 2003; 2:347–360. [PubMed: 12750738]
6. Kopecek J, Kopeckova P, Minko T, Lu Z. HPMA copolymer-anticancer drug conjugates: design, activity, and mechanism of action. Eur J Pharm Biopharm. 2000; 50:61–81. [PubMed: 10840193]
7. Torchilin VP. Affinity liposomes in vivo: factors influencing target accumulation. J Mol Recognit. 1996; 9:335–346. [PubMed: 9174907]
8. Bae YH, Park K. Targeted drug delivery to tumors: Myths, reality and possibility. J Control Release. 2011; 153:198–205. [PubMed: 21663778]
9. Lammers T, Hennink WE, Storm G. Tumour-targeted nanomedicines: principles and practice. Br J Cancer. 2008; 99:392–397. [PubMed: 18648371]
10. Maeda H, Matsumura Y. Tumoritropic and Lymphotropic Principles of Macromolecular Drugs. Crit Rev Ther Drug Carr Syst. 1989; 6:193–210.
11. Matsumura Y, Maeda H. A New Concept for Macromolecular Therapeutics in Cancer-Chemotherapy - Mechanism of Tumoritropic Accumulation of Proteins and the Antitumor Agent Smancs. Cancer Res. 1986; 46:6387–6392. [PubMed: 2946403]
12. Seymour LW. Passive Tumor Targeting of Soluble Macromolecules and Drug Conjugates. Crit Rev Ther Drug Carr Syst. 1992; 9:135–187.
13. Lammers T, Kiessling F, Hennink WE, Storm G. Drug targeting to tumors: Principles, pitfalls and (pre-) clinical progress. J Control Release. 2011
14. Paolino, D.; Fresta, M.; Sinha, P.; Ferrari, A. Drug Delivery Systems. In: Webster, JG., editor. The Encyclopedia of Medical Devices and Instrumentation. Wiley & Sons Inc; 2006. p. 437-495.
15. Kingham TP, D'Angelica M, Kemeny NE. Role of intra-arterial hepatic chemotherapy in the treatment of colorectal cancer metastases. J Surg Oncol. 2010; 102:988–995. [PubMed: 21166003]
16. Meric F, Patt YZ, Curley SA, Chase J, Roh MS, Vauthey JN, Ellis LM. Surgery after downstaging of unresectable hepatic tumors with intra-arterial chemotherapy. Ann Surg Oncol. 2000; 7:490–495. [PubMed: 10947016]
17. Lewandowski RJ, Geschwind JF, Liapi E, Salem R. Transcatheter intraarterial therapies: rationale and overview. Radiology. 2011; 259:641–657. [PubMed: 21602502]
18. Chen HS, Gross JF. Intra-arterial infusion of anticancer drugs: theoretic aspects of drug delivery and review of responses. Cancer Treat Rep. 1980; 64:31–40. [PubMed: 6155210]
19. Collins JM. Pharmacologic rationale for regional drug delivery. J Clin Oncol. 1984; 2:498–504. [PubMed: 6547166]
20. Ensminger WD, Gyves JW. Clinical pharmacology of hepatic arterial chemotherapy. Semin Oncol. 1983; 10:176–182. [PubMed: 6346495]
21. Yamada R, Nakatsuka H, Nakamura K, Sato M, Itami M, Kobayashi N, Minakuchi K, Onoyama T, Kanno T, Monna T, Yamamoto S. Hepatic artery embolization in 32 patients with unresectable hepatoma. Osaka City Med J. 1980; 26:81–96. [PubMed: 6170035]
22. Marelli L, Stigliano R, Triantos C, Senzolo M, Cholongitas E, Davies N, Tibballs J, Meyer T, Patch DW, Burroughs AK. Transarterial therapy for hepatocellular carcinoma: which technique is

more effective? A systematic review of cohort and randomized studies. Cardiovascular and interventional radiology. 2007; 30:6–25. [PubMed: 17103105]

23. Brown DB, Gould JE, Gervais DA, Goldberg SN, Murthy R, Millward SF, Rilling WS, Geschwind JF, Salem R, Vedantham S, Cardella JF, Soulen MCC. Society of Interventional Radiology Technology Assessment, A. the International Working Group on Image-Guided Tumor, Transcatheter therapy for hepatic malignancy: standardization of terminology and reporting criteria. J Vasc Interv Radiol. 2009; 20:S425–434. [PubMed: 19560030]
24. Liapi E, Geschwind JF. Transcatheter arterial chemoembolization for liver cancer: is it time to distinguish conventional from drug-eluting chemoembolization? Cardiovasc Intervent Radiol. 2011; 34:37–49. [PubMed: 21069333]
25. Konno T, Maeda H, Iwai K, Tashiro S, Maki S, Morinaga T, Mochinaga M, Hiraoka T, Yokoyama I. Effect of arterial administration of high-molecular-weight anticancer agent SMANCS with lipid lymphographic agent on hepatoma: a preliminary report. Eur J Cancer Clin Oncol. 1983; 19:1053–1065. [PubMed: 6311559]
26. Maluccio MA, Covey AM, Porat LB, Schubert J, Brody LA, Sofocleous CT, Getrajdman GI, Jarnagin W, Dematteo R, Blumgart LH, Fong Y, Brown KT. Transcatheter arterial embolization with only particles for the treatment of unresectable hepatocellular carcinoma. J Vasc Interv Radiol. 2008; 19:862–869. [PubMed: 18503900]
27. Nakamura H, Hashimoto T, Oi H, Sawada S. Transcatheter oily chemoembolization of hepatocellular carcinoma. Radiology. 1989; 170:783. [PubMed: 2536946]
28. Sasaki Y, Imaoka S, Kasugai H, Fujita M, Kawamoto S, Ishiguro S, Kojima J, Ishikawa O, Ohigashi H, Furukawa H. A new approach to chemoembolization therapy for hepatoma using ethiodized oil, cisplatin, and gelatin sponge. Cancer. 1987; 60
29. Brown DB, Geschwind JFH, Soulen MC, Millward SF, Sacks D. Society of Interventional Radiology position statement on chemoembolization of hepatic malignancies. J Vasc Interv Radiol. 2006; 17:217–223. [PubMed: 16517767]
30. Geschwind JFH, Ramsey DE, van der Wal BCH, Kobeiter H, Juluru K, Hartnell GG, Choti MA. Transcatheter arterial chemoembolization of liver tumors: effects of embolization protocol on injectable volume of chemotherapy and subsequent arterial patency. Cardiovasc Intervent Radiol. 2003; 26:111–117. [PubMed: 12616414]
31. Brown DB, Pilgram TK, Darcy MD, Fundakowski CE, Lisker-Melman M, Chapman WC, Crippin JS. Hepatic arterial chemoembolization for hepatocellular carcinoma: comparison of survival rates with different embolic agents. J Vasc Interv Radiol. 2005; 16:1661–1666. [PubMed: 16371533]
32. Lewandowski RJ, Wang D, Gehl J, Atassi B, Ryu RK, Sato K, Nemcek AA Jr, Miller FH, Mulcahy MF, Kulik L, Larson AC, Salem R, Omary RA. A comparison of chemoembolization endpoints using angiographic versus transcatheter intraarterial perfusion/MR imaging monitoring. J Vasc Interv Radiol. 2007; 18:1249–1257. [PubMed: 17911515]
33. Biondi M, Fusco S, Lewis AL, Netti PA. New Insights into the Mechanisms of the Interactions Between Doxorubicin and the Ion-Exchange Hydrogel DC Bead for Use in Transarterial Chemoembolization (TACE). J Biomater Sci Polym Ed. 2011
34. Gonzalez MV, Tang Y, Phillips GJ, Lloyd AW, Hall B, Stratford PW, Lewis AL. Doxorubicin eluting beads-2: methods for evaluating drug elution and in-vitro:in-vivo correlation. J Mater Sci Mater Med. 2007; 19:767–775. [PubMed: 17653626]
35. Lewis AL. DC Bead(TM): a major development in the toolbox for the interventional oncologist. Expert Rev Med Devices. 2009; 6:389–400. [PubMed: 19572794]
36. Lewis AL, Gonzalez MV, Leppard SW, Brown JE, Stratford PW, Phillips GJ, Lloyd AW. Doxorubicin eluting beads - 1: effects of drug loading on bead characteristics and drug distribution. J Mater Sci Mater Med. 2007; 18:1691–1699. [PubMed: 17483878]
37. Lewis AL, Gonzalez MV, Lloyd AW, Hall B, Tang Y, Willis SL, Leppard SW, Wolfenden LC, Palmer RR, Stratford PW. DC bead: in vitro characterization of a drug-delivery device for transarterial chemoembolization. J Vasc Interv Radiol. 2006; 17:335–342. [PubMed: 16517780]
38. Taylor RR, Tang Y, Gonzalez MV, Stratford PW, Lewis AL. Irinotecan drug eluting beads for use in chemoembolization: in vitro and in vivo evaluation of drug release properties. Eur J Pharm Sci. 2007; 30:7–14. [PubMed: 17030118]

39. Tomlinson E. Microsphere delivery systems for drug targeting and controlled release. Int J Pharm Tech Prod Mfr. 1983; 4:49–57.
40. Kerr DJ. Microparticulate drug delivery systems as an adjunct to cancer treatment. Cancer Drug Deliv. 1987; 4:55–61. [PubMed: 3300944]
41. Lewis, AL. Drug eluting beads in the treatment of liver cancer. In: Lewis, AL., editor. Drug-Device Combination Products Delivery Technologies and Applications. Woodhead publishing ltd; Cambridge: 2010. p. 154-189.
42. Poon RTP, Tso WK, Pang RWC, Ng KKC, Woo R, Tai KS, Fan ST. A Phase I/II Trial of Chemoembolization for Hepatocellular Carcinoma Using a Novel Intra-Arterial Drug-Eluting Bead. Clinical Gastroenterology and Hepatology. 2007; 5:1100–1108. [PubMed: 17627902]
43. Varela M, Real MI, Burrel M, Forner A, Sala M, Brunet M, Ayuso C, Castells L, MontaÃ±Ã¡ X, Llovet JM. Chemoembolization of hepatocellular carcinoma with drug eluting beads: efficacy and doxorubicin pharmacokinetics. J Hepatol. 2007; 46:474–481. [PubMed: 17239480]
44. Lewis AL, Holden RR. DC Bead embolic drug-eluting bead: clinical application in the locoregional treatment of tumours. Expert Opin Drug Deliv. 2011; 8:153–169. [PubMed: 21222553]
45. Lee KH, Liapi EA, Cornell C, Reb P, Buijs M, Vossen JA, Ventura VP, Geschwind JF. Doxorubicin-loaded QuadraSphere microspheres: plasma pharmacokinetics and intratumoral drug concentration in an animal model of liver cancer. Cardiovasc Intervent Radiol. 2010; 33:576–582. [PubMed: 20087738]
46. Jordan O, Denys A, De Baere T, Boulens N, Doelker E. Comparative study of chemoembolization loadable beads: in vitro drug release and physical properties of DC bead and hepasphere loaded with doxorubicin and irinotecan. J Vasc Interv Radiol. 2010; 21:1084–1090. [PubMed: 20610183]
47. Gupta S, Wright KC, Ensor J, Van Pelt CS, Dixon KA, Kundra V. Hepatic arterial embolization with Doxorubicin-loaded superabsorbent polymer microspheres in a rabbit liver tumor model. Cardiovascular and interventional radiology. 2011; 34:1021–1030. [PubMed: 21479746]
48. van Malenstein H, Maleux G, Vandecaveye V, Heye S, Laleman W, van Pelt J, Vaninbroukx J, Nevens F, Verslype C. A randomized phase II study of drug-eluting beads versus transarterial chemoembolization for unresectable hepatocellular carcinoma. Onkologie. 2011; 34:368–376. [PubMed: 21734423]
49. Grosso M, Vignali C, Quaretti P, Nicolini A, Melchiorre F, Gallarato G, Bargellini I, Petruzzi P, Massa Saluzzo C, Crespi S, Sarti I. Transarterial chemoembolization for hepatocellular carcinoma with drug-eluting microspheres: preliminary results from an Italian multicentre study. Cardiovasc Intervent Radiol. 2008; 31:1141–1149. [PubMed: 18696150]
50. Seki A, Hori S, Kobayashi K, Narumiya S. Transcatheter arterial chemoembolization with epirubicin-loaded superabsorbent polymer microspheres for 135 hepatocellular carcinoma patients: single-center experience. Cardiovasc Intervent Radiol. 2011; 34:557–565. [PubMed: 20821211]
51. Llovet JM, Real MI, MontaÃ±a X, Planas R, Coll S, Aponte J, Ayuso C, Sala M, Muchart J, SolÃ R. Arterial embolisation or chemoembolisation versus symptomatic treatment in patients with unresectable hepatocellular carcinoma: a randomised controlled trial. The Lancet. 2002; 359:1734–1739.
52. Lo CM, Ngan H, Tso WK, Liu CL, Lam CM, Poon RTP, Fan ST, Wong J. Randomized controlled trial of transarterial lipiodol chemoembolization for unresectable hepatocellular carcinoma. Hepatology. 2002; 35
53. Hong K, Khwaja A, Liapi E, Torbenson MS, Georgiades CS, Geschwind JF. New intra-arterial drug delivery system for the treatment of liver cancer: preclinical assessment in a rabbit model of liver cancer. Clin Cancer Res. 2006; 12:2563–2567. [PubMed: 16638866]
54. Lammer J, Malagari K, Vogl T, Pilleul F, Denys A, Watkinson A, Pitton M, Sergent G, Pfammatter T, Terraz S, Benhamou Y, Avajon Y, Gruenberger T, Pomoni M, Langenberger H, Schuchmann M, Dumortier J, Mueller C, Chevallier P, Lencioni R. Prospective randomized study of doxorubicin-eluting-bead embolization in the treatment of hepatocellular carcinoma: results of the PRECISION V study. Cardiovasc Intervent Radiol. 2010; 33:41–52. [PubMed: 19908093]
55. Dhanasekaran R, Kooby DA, Staley CA, Kauh JS, Khanna V, Kim HS. Comparison of conventional transarterial chemoembolization (TACE) and chemoembolization with doxorubicin

drug eluting beads (DEB) for unresectable hepatocelluar carcinoma (HCC). J Surg Oncol. 2010; 101:476–480. [PubMed: 20213741]

56. Johnson PJ, Kalayci C, Dobbs N, Raby N, Metivier EM, Summers L, Harper P, Williams R. Pharmacokinetics and toxicity of intraarterial adriamycin for hepatocellular carcinoma: effect of coadministration of lipiodol. Journal of hepatology. 1991; 13:120–127. [PubMed: 1655867]
57. Gaba RC, Baumgarten S, Omene BO, van Breemen RB, Garcia KD, Larson AC, Omary RA. Ethiodized Oil Uptake Does Not Predict Doxorubicin Drug Delivery after Chemoembolization in VX2 Liver Tumors. J Vasc Interv Radiol. 2011
58. Malagari K, Pomoni M, Kelekis A, Pomoni A, Dourakis S, Spyridopoulos T, Moschouris H, Emmanouil E, Rizos S, Kelekis D. Prospective randomized comparison of chemoembolization with doxorubicin-eluting beads and bland embolization with BeadBlock for hepatocellular carcinoma. Cardiovasc Intervent Radiol. 2010; 33:541–551. [PubMed: 19937027]
59. Nicolini A, Martinetti L, Crespi S, Maggioni M, Sangiovanni A. Transarterial chemoembolization with epirubicin-eluting beads versus transarterial embolization before liver transplantation for hepatocellular carcinoma. Journal of vascular and interventional radiology : JVIR. 2010; 21:327–332. [PubMed: 20097098]
60. Lencioni R, Crocetti L, Petruzzi P, Vignali C, Bozzi E, Della Pina C, Bargellini I, Cioni D, Oliveri F, De Simone P, Bartolozzi C, Brunetto M, Filipponi F. Doxorubicin-eluting bead-enhanced radiofrequency ablation of hepatocellular carcinoma: a pilot clinical study. Journal of hepatology. 2008; 49:217–222. [PubMed: 18486261]
61. Gadaleta C, Catino A, Ranieri G, Fazio V, Gadaleta-Caldarola G, Cramarossa A, Armenise F, Canniello E, Vinciarelli G, Laricchia G, Mattioli V. Single-step therapy -- feasibility and safety of simultaneous transarterial chemoembolization and radiofrequency ablation for hepatic malignancies. In Vivo. 2009; 23:813–820. [PubMed: 19779117]
62. Aliberti C, Benea G, Tilli M, Fiorentini G. Chemoembolization (TACE) of unresectable intrahepatic cholangiocarcinoma with slow-release doxorubicin-eluting beads: preliminary results. Cardiovasc Intervent Radiol. 2008; 31:883–888. [PubMed: 18478290]
63. Fiorentini G, Aliberti C, Turrisi G, Del Conte A, Rossi S, Benea G, Giovanis P. Intraarterial hepatic chemoembolization of liver metastases from colorectal cancer adopting irinotecan-eluting beads: results of a phase II clinical study. In Vivo. 2007; 21:1085–1091. [PubMed: 18210761]
64. Martin RC, Joshi J, Robbins K, Tomalty D, O'Hara R, Tatum C. Transarterial Chemoembolization of Metastatic Colorectal Carcinoma with Drug-Eluting Beads, Irinotecan (DEBIRI): Multi-Institutional Registry. J Oncol. 2009; 2009:539795. [PubMed: 19888427]
65. Fiorentini. in press.
66. Bower M, Metzger T, Robbins K, Tomalty D, Valek V, Boudny J, Andrasina T, Tatum C, Martin RC. Surgical downstaging and neo-adjuvant therapy in metastatic colorectal carcinoma with irinotecan drug-eluting beads: a multi-institutional study. HPB (Oxford). 2010; 12:31–36. [PubMed: 20495642]
67. de Baere T, Deschamps F, Teriitheau C, Rao P, Conengrapht K, Schlumberger M, Leboulleux S, Baudin E, Hechellhammer L. Transarterial chemoembolization of liver metastases from well differentiated gastroenteropancreatic endocrine tumors with doxorubicin-eluting beads: preliminary results. J Vasc Interv Radiol. 2008; 19:855–861. [PubMed: 18503899]
68. Schiffman SC, Metzger T, Dubel G, Andrasina T, Kralj I, Tatum C, McMasters KM, Scoggins CR, Martin RC. Precision hepatic arterial irinotecan therapy in the treatment of unresectable intrahepatic cholangiocellular carcinoma: optimal tolerance and prolonged overall survival. Annals of surgical oncology. 2011; 18:431–438. [PubMed: 20862554]
69. Fiorentini G, Aliberti C, Del Conte A, Tilli M, Rossi S, Ballardini P, Turrisi G, Benea G. Intra-arterial hepatic chemoembolization (TACE) of liver metastases from ocular melanoma with slow-release irinotecan-eluting beads. Early results of a phase II clinical study. In Vivo. 2009; 23:131–137. [PubMed: 19368137]
70. Laurent A, Wassef M, Namur J, Ghegediban H, Pelage JP. Arterial distribution of calibrated tris-acryl gelatin and polyvinyl alcohol embolization microspheres in sheep uterus. Cardiovascular and interventional radiology. 2010; 33:995–1000. [PubMed: 20300751]

71. Laurent A, Wassef M, Chapot R, Houdart E, Merland JJ. Location of vessel occlusion of calibrated tris-acryl gelatin microspheres for tumor and arteriovenous malformation embolization. Journal of vascular and interventional radiology : JVIR. 2004; 15:491–496. [PubMed: 15126660]
72. Tadavarthy SM, Moller JH, Amplatz K. Polyvinyl alcohol (Ivalon)--a new embolic material. Am J Roentgenol Radium Ther Nucl Med. 1975; 125:609–616.
73. Namur J, Wassef M, Millot JM, Lewis AL, Manfait M, Laurent A. Drug-eluting beads for liver embolization: concentration of doxorubicin in tissue and in beads in a pig model. J Vasc Interv Radiol. 2010; 21:259–267. [PubMed: 20123210]
74. Namur J, Wassef M, Pelage JP, Lewis A, Manfait M, Laurent A. Infrared microspectroscopy analysis of ibuprofen release from drug eluting beads in uterine tissue. J Control Release. 2009; 135:198–202. [PubMed: 19367683]
75. Namur J, Citron SJ, Sellers MT, Dupuis MH, Wassef M, Manfait M, Laurent A. Embolization of hepatocellular carcinoma with drug-eluting beads: doxorubicin tissue concentration and distribution in patient liver explants. J Hepatol. 2011; 55:1332–1338. [PubMed: 21703190]
76. http://www.clinicaltrials.gov/, in.
77. Dreher MR, Sharma KV, Woods DL, Reddy G, Tang Y, Pritchard WF, Chiesa OA, Karanian JW, Esparza JA, Donahue D, Levy EB, Willis SL, Lewis AL, Wood BJ. Radiopaque Drug-Eluting Beads for Transcatheter Embolotherapy: Experimental Study of Drug Penetration and Coverage in Swine. J Vasc Interv Radiol. 2011
78. Gupta T, Virmani S, Neidt TM, Szolc-Kowalska B, Sato KT, Ryu RK, Lewandowski RJ, Gates VL, Woloschak GE, Salem R, Omary RA, Larson AC. MR tracking of iron-labeled glass radioembolization microspheres during transcatheter delivery to rabbit VX2 liver tumors: feasibility study. Radiology. 2008; 249:845–854. [PubMed: 18840788]
79. Lee KH, Liapi E, Vossen JA, Buijs M, Ventura VP, Georgiades C, Hong K, Kamel I, Torbenson MS, Geschwind JFH. Distribution of iron oxide-containing Embosphere particles after transcatheter arterial embolization in an animal model of liver cancer: Evaluation with MR Imaging and implication for therapy. J Vasc Interv Radiol. 2008; 19:1490–1496. [PubMed: 18755602]
80. Namur J, Chapot R, Pelage JP, Wassef M, Langevin F, Labarre D, Laurent A. MR imaging detection of superparamagnetic iron oxide loaded tris-acryl embolization microspheres. J Vasc Interv Radiol. 2007; 18:1287–1295. [PubMed: 17911520]
81. Wilson MW, Fidelman N, Weber OM, Martin AJ, Gordon RL, LaBerge JM, Kerlan RK Jr, Wolanske KA, Saeed M. Experimental renal artery embolization in a combined MR imaging/angiographic unit. J Vasc Interv Radiol. 2003; 14:1169–1175. [PubMed: 14514809]
82. Cilliers R, Song Y, Kohlmeir EK, Larson AC, Omary RA, Meade TJ. Modification of embolic-PVA particles with MR contrast agents. Magnetic resonance in medicine : official journal of the Society of Magnetic Resonance in Medicine/Society o. 2008; 59:898–902.
83. Seevinck PR, Seppenwoolde JH, Zwanenburg JJ, Nijsen JF, Bakker CJ. FID sampling superior to spin-echo sampling for T2*-based quantification of holmium-loaded microspheres: theory and experiment. Magnetic resonance in medicine : official journal of the Society of Magnetic Resonance in Medicine/Society o. 2008; 60:1466–1476.
84. Saralidze K, van Hooy-Corstjens CS, Koole LH, Knetsch ML. New acrylic microspheres for arterial embolization: combining radiopacity for precise localization with immobilized thrombin to trigger local blood coagulation. Biomaterials. 2007; 28:2457–2464. [PubMed: 17257667]
85. Sharma KV, Dreher MR, Tang Y, Pritchard W, Chiesa OA, Karanian J, Peregoy J, Orandi B, Woods D, Donahue D, Esparza J, Jones G, Willis SL, Lewis AL, Wood BJ. Development of “imageable” beads for transcatheter embolotherapy. J Vasc Interv Radiol. 2010; 21:865–876. [PubMed: 20494290]
86. Bartling SH, Budjan J, Aviv H, Haneder S, Kraenzlin B, Michaely H, Margel S, Diehl S, Semmler W, Gretz N, Schonberg SO, Sadick M. First multimodal embolization particles visible on x-ray/computed tomography and magnetic resonance imaging. Invest Radiol. 2011; 46:178–186. [PubMed: 21263332]

87. Fukumura D, Yuan F, Monsky WL, Chen Y, Jain RK. Effect of host microenvironment on the microcirculation of human colon adenocarcinoma. The American journal of pathology. 1997; 151:679–688. [PubMed: 9284816]

88. Tong RT, Boucher Y, Kozin SV, Winkler F, Hicklin DJ, Jain RK. Vascular normalization by vascular endothelial growth factor receptor 2 blockade induces a pressure gradient across the vasculature and improves drug penetration in tumors. Cancer Res. 2004; 64:3731–3736. [PubMed: 15172975]

89. Vakoc BJ, Lanning RM, Tyrrell JA, Padera TP, Bartlett LA, Stylianopoulos T, Munn LL, Tearney GJ, Fukumura D, Jain RK, Bouma BE. Three-dimensional microscopy of the tumor microenvironment in vivo using optical frequency domain imaging. Nature medicine. 2009; 15:1219–1223.

90. Yuan F, Chen Y, Dellian M, Safabakhsh N, Ferrara N, Jain RK. Time-dependent vascular regression and permeability changes in established human tumor xenografts induced by an anti-vascular endothelial growth factor/vascular permeability factor antibody. Proceedings of the National Academy of Sciences of the United States of America. 1996; 93:14765–14770. [PubMed: 8962129]

91. Sharma KV, Dreher M, Rudnick N, Friman O, Ali M, Levy E, Tabriz D, Wood BJ, Haemmerich D. Abstract No. 286: Quantification of blood flow changes observed during DEB-TACE: A tool for standardization and optimization. Journal of Vascular and Interventional Radiology. 2011; 22:S120–S121.

92. Deschamps F, Solomon SB, Thornton RH, Rao P, Hakime A, Kuoch V, de Baere T. Computed Analysis of Three-Dimensional Cone-Beam Computed Tomography Angiography for Determination of Tumor-Feeding Vessels During Chemoembolization of Liver Tumor: A Pilot Study. Cardiovasc Intervent Radiol. 2010

93. Loffroy R, Lin M, Rao P, Bhagat N, Noordhoek N, Radaelli A, Blijd J, Geschwind JF. Comparing the Detectability of Hepatocellular Carcinoma by C-Arm Dual-Phase Cone-Beam Computed Tomography During Hepatic Arteriography With Conventional Contrast-Enhanced Magnetic Resonance Imaging. Cardiovasc Intervent Radiol. 2011

94. Wallace MJ, Kuo MD, Glaiberman C, Binkert CA, Orth RC, Soulez G. Three-dimensional C-arm cone-beam CT: applications in the interventional suite. J Vasc Interv Radiol. 2009; 20:S523–537. [PubMed: 19560037]

95. Solomon SB, Thornton R, Deschamps F, Pichon E, Trousset Y, Grimaud M, Houdant S, Getrajdman G, De Baere T. A Treatment Planning System for Transcatheter Hepatic Therapies: Pilot Study. Journal of Interventional Oncology. 2008; 1:12–18.

96. Wood BJ, Ramkaransingh JR, Fojo T, Walther MM, Libutti SK. Percutaneous tumor ablation with radiofrequency. Cancer. 2002; 94:443–451. [PubMed: 11900230]

97. Pawlik TM, Reyes DK, Cosgrove D, Kamel IR, Bhagat N, Geschwind JF. Phase II Trial of Sorafenib Combined With Concurrent Transarterial Chemoembolization With Drug-Eluting Beads for Hepatocellular Carcinoma. Journal of clinical oncology : official journal of the American Society of Clinical Oncology. 2011

98. Yang W, Chen MH, Wang MQ, Cui M, Gao W, Wu W, Wu JY, Dai Y, Yan K. Combination therapy of radiofrequency ablation and transarterial chemoembolization in recurrent hepatocellular carcinoma after hepatectomy compared with single treatment. Hepatol Res. 2009; 39:231–240. [PubMed: 19054154]

99. Lu DS, Raman SS, Vodopich DJ, Wang M, Sayre J, Lassman C. Effect of vessel size on creation of hepatic radiofrequency lesions in pigs: assessment of the “heat sink” effect. AJR Am J Roentgenol. 2002; 178:47–51. [PubMed: 11756085]

100. Schutt DJ, Haemmerich D. Effects of variation in perfusion rates and of perfusion models in computational models of radio frequency tumor ablation. Med Phys. 2008; 35:3462–3470. [PubMed: 18777906]

101. Lencioni R. Loco-regional treatment of hepatocellular carcinoma in the era of molecular targeted therapies. Oncology. 2010; 78(Suppl 1):107–112. [PubMed: 20616592]

102. Rhee TK, Young JY, Larson AC, Haines GK 3rd, Sato KT, Salem R, Mulcahy MF, Kulik LM, Paunesku T, Woloschak GE, Omary RA. Effect of transcatheter arterial embolization on levels of

hypoxia-inducible factor-1alpha in rabbit VX2 liver tumors. Journal of vascular and interventional radiology : JVIR. 2007; 18:639–645. [PubMed: 17494846]

103. Liang B, Zheng CS, Feng GS, Wu HP, Wang Y, Zhao H, Qian J, Liang HM. Correlation of hypoxia-inducible factor 1alpha with angiogenesis in liver tumors after transcatheter arterial embolization in an animal model. Cardiovascular and interventional radiology. 2010; 33:806–812. [PubMed: 19937023]
104. Bowyer, C.; Forster, R.; Lewis, A.; Phillips, G.; Lloyd, AW.; Macfarlane, W. An Evaluation of Doxorubicin, Rapamycin and Combinations Thereof in Drug Eluting Beads using in vitro and in vivo HEPG2 Liver Cancer Models. Abstracts from 4th ILCA Conference; 2010. p. 30
105. Forster R, Tang Y, Bowyer C, Lloyd AW, Macfarlane W, Phillips G, Lewis AL. Development of a combination drug eluting bead: towards enhanced efficacy for locoregional therapies. Anticancer Drugs. In press.
106. Weber C, Pohl S, Poertner R, Pino-Grace P, Freimark D, Wallrapp C, Geigle P, Czermak P. Production process for stem cell based therapeutic implants: expansion of the production cell line and cultivation of encapsulated cells. Adv Biochem Eng Biotechnol. 2010; 123:143–162. [PubMed: 20091287]
107. Houtgraaf JH. Feasibility of intracoronary GLP-1 eluting CellBead™ infusion in acute myocardial infarction. Cell transplantation. (in press).
108. Baltes S, Freund I, Lewis AL, Nolte I, Brinker T. Doxorubicin and irinotecan drug-eluting beads for treatment of glioma: a pilot study in a rat model. Journal of materials science Materials in medicine. 2010; 21:1393–1402. [PubMed: 20162337]
109. Held N, Lewis AL, Hedrich HJ, Brinker T, Glage S. A safety and toxicity assessment of the administration of multiple intracerebral injections of irinotecan or doxorubicin drug-eluting beads. Clin Transl Oncol. 2011; 13:742–746. [PubMed: 21975337]
110. Vinchon-Petit S, Jarnet D, Michalak S, Lewis A, Benoit JP, Menei P. Local implantation of doxorubicin drug eluting beads in rat glioma. Int J Pharm. 2010; 402:184–189. [PubMed: 20863875]
111. Forster RE, Small SA, Tang Y, Heaysman CL, Lloyd AW, Macfarlane W, Phillips GJ, Antonijevic MD, Lewis AL. Comparison of DC Bead-irinotecan and DC Bead-topotecan drug eluting beads for use in locoregional drug delivery to treat pancreatic cancer. Journal of materials science Materials in medicine. 2010; 21:2683–2690. [PubMed: 20563626]
112. Karaca C, Cizginer S, Konuk Y, Kambadakone A, Turner BG, Mino-Kenudson M, Sahani DV, Macfarlane C, Brugge W. Feasibility of EUS-guided injection of irinotecan-loaded microspheres into the swine pancreas. Gastrointest Endosc. 2011; 73:603–606. [PubMed: 21238959]
113. Keese M, Gasimova L, Schwenke K, Yagublu V, Shang E, Faissner R, Lewis A, Samel S, Lohr M. Doxorubicin and mitoxantrone drug eluting beads for the treatment of experimental peritoneal carcinomatosis in colorectal cancer. Int J Cancer. 2009; 124:2701–2708. [PubMed: 19165866]

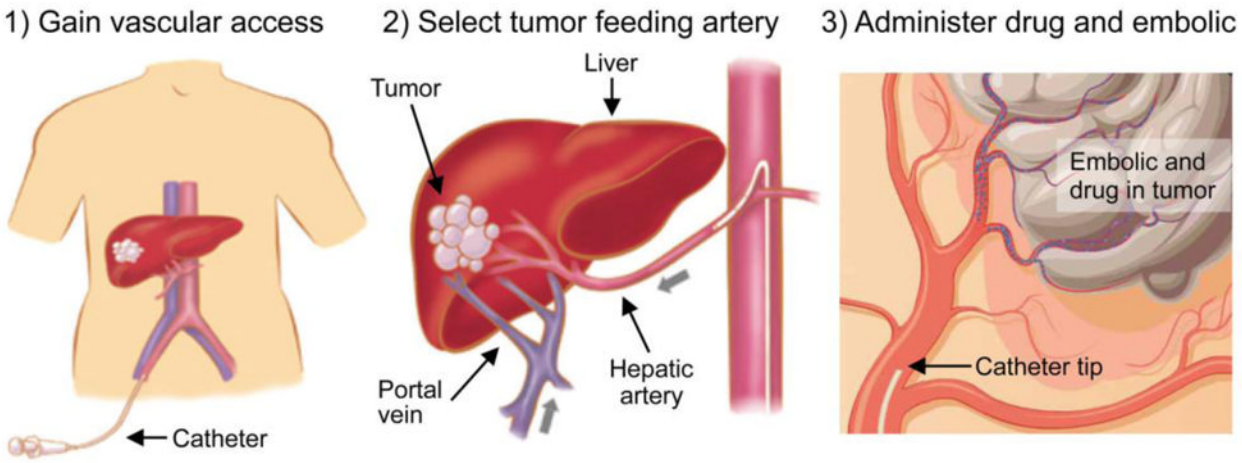

Figure 1.
Schematic describing the principles of TACE. Access is gained in the femoral artery (left) and a hepatic artery is selected by use of a guidewire and a catheter (middle). A microcatheter is then often positioned a tumor feeding artery (right). From this location, TACE is performed by infusing a mixture of chemotherapeutics and embolic agents (right).

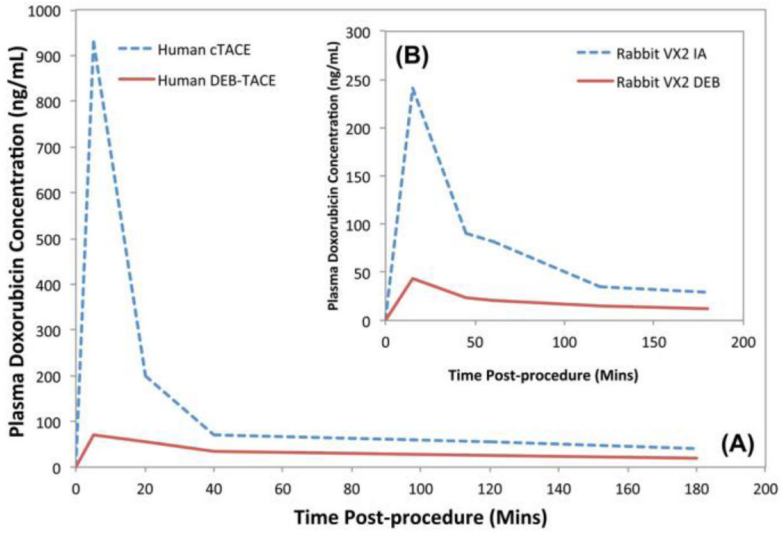

Figure 2.

Comparison of doxorubicin pharmacokinetic (PK) profile following conventional Lipiodol-based TACE (cTACE), intra-arterial infusion (IA) and DEB-TACE using doxorubicin. (A) Human plasma doxorubicin concentration. (B) Rabbit plasma doxorubicin concentration in a rabbit Vx-2 tumor model. Note the similarities between (A) and (B) indicating the useful predictive nature of the animal model for systemic drug levels obtained using DEBs. Direct comparison between cTACE in part A and IA in part B is not possible. From [44] with permission.

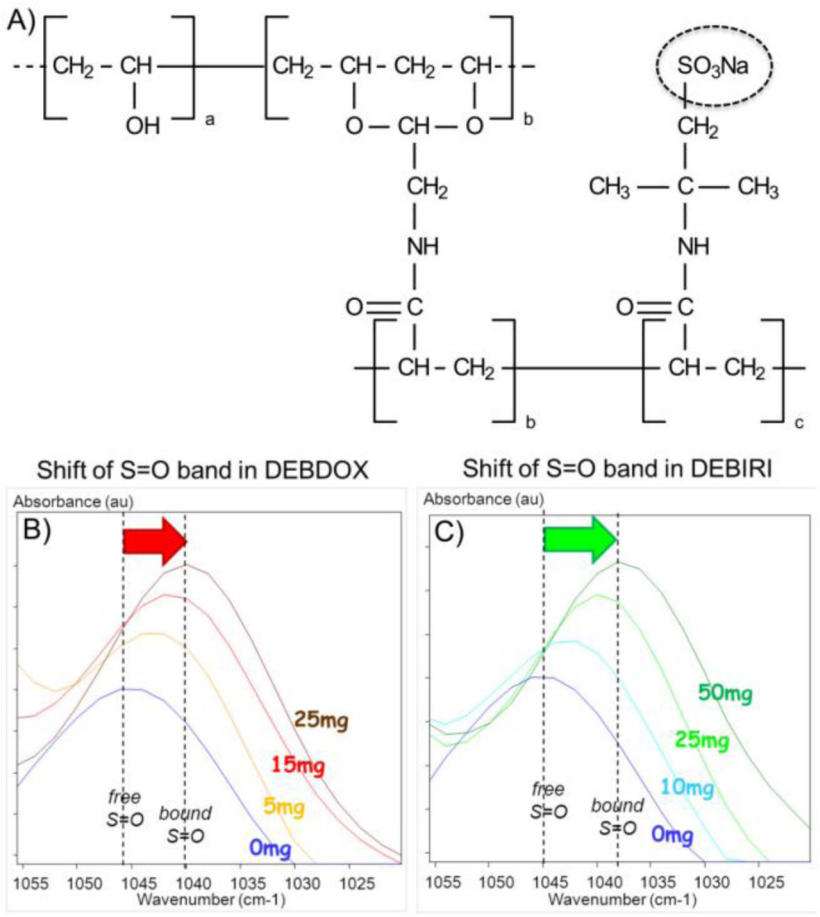

Figure 3.

A) Chemical structure of the sulfonate-modified polyvinyl alcohol hydrogel polymer used in the fabrication of DC Bead. B) and C) Demonstration of the ionic interaction between the sulfonate groups in DEB (see dashed circle in A) with doxorubicin (B) or irinotecan (C) using Fourier Transform Infrared Microscopy. Note the shift in the position of the S=O stretching absorption from higher to lower wavenumber with increasing concentration of drug bound within the system, denoting a shift from free to bound S=O groups. B and C courtesy of Dr. J. Namur.

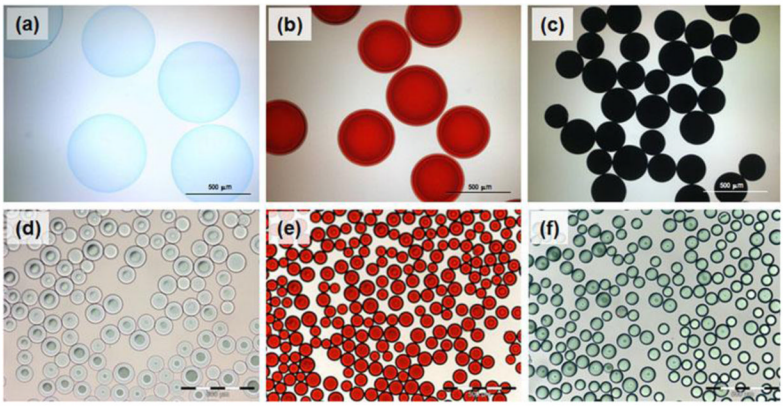

Figure 4.

Optical micrographs of DEBs. (a) Unloaded 500–700 μm DEB; (b) Doxorubicin (18.2 mg/mL) loaded 500–700 μm DEB; (c) Mitoxantrone (19.8 mg/mL) loaded 500–700 μm DEB. Note the effect of mono or divalent drug binding on bead size and the color imparted by the drug. (d) Unloaded DEB (70–150 μm); (e) Doxorubicin (37.5 mg/mL) loaded DEB (70–150 μm); (f) Irinotecan (50 mg/mL) loaded DEB (70–150 μm). Note that these DEBs (d, e and f) are much smaller than that used to conduct the early Phase I/II clinical studies with DEB (b).

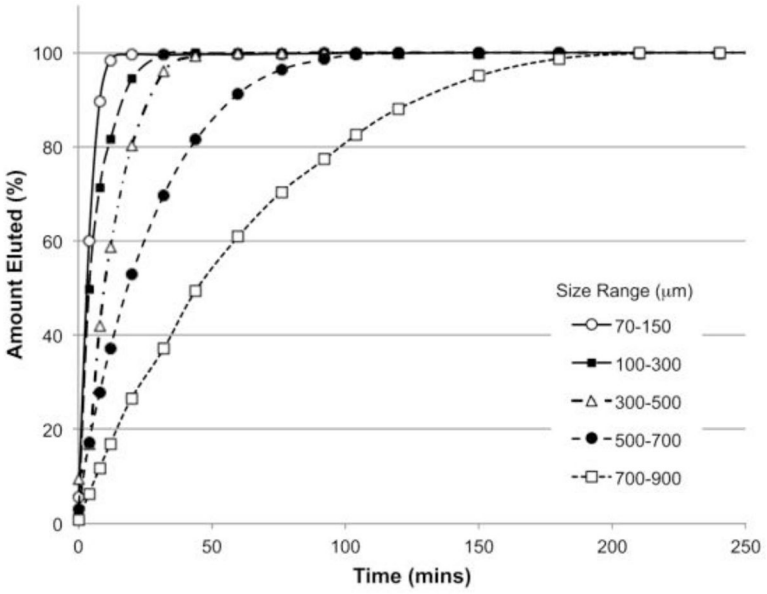

Figure 5.

Comparative release of 25 mg/mL doxorubicin from the various DEB size ranges as measured by a USP II method using PBS as elution medium under sink conditions at 25°C. Release is a function of the surface area to volume ratio. Under these conditions, release can be modeled as approximating to first order [34]. Whilst useful for product development and QC purposes, this elution test is non-predictive for *in vivo* drug release, which has been demonstrated to occur over many weeks to months [73, 75].

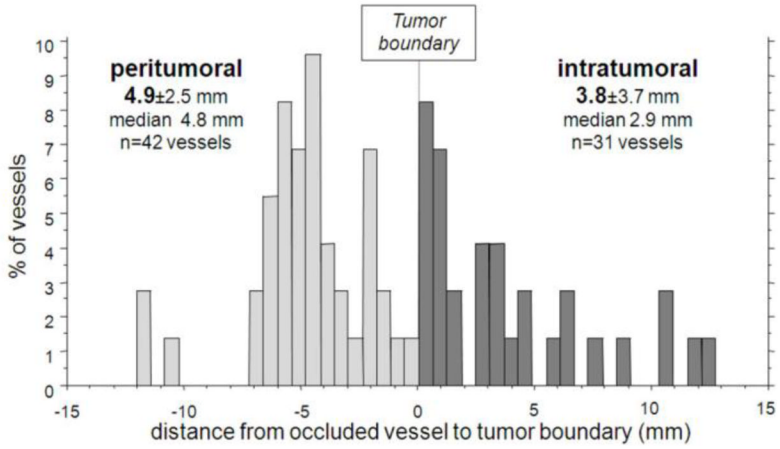

Figure 6.
Distribution of DEB inside or at the periphery of the tumor nodule in a patient transplanted at 8 hours after DEB-TACE. From [75] with permission.

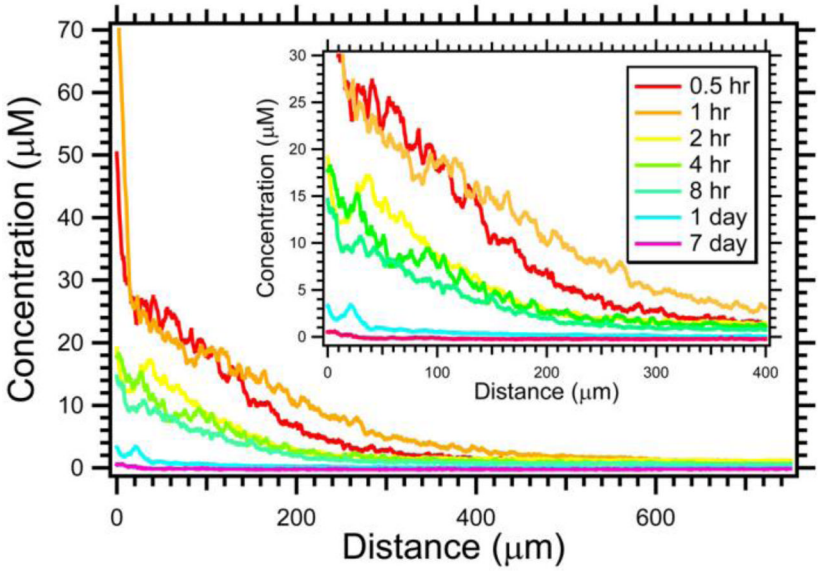

Figure 7.

Penetration of doxorubicin in swine liver for 100–300 μm radiopaque drug-eluting beads. Insert displays a magnified view of the same data to better appreciate the influence of time (N = 14–34). These DEBs were made radiopaque by the inclusion of Lipiodol inside the DEBs. From [77] with permission.

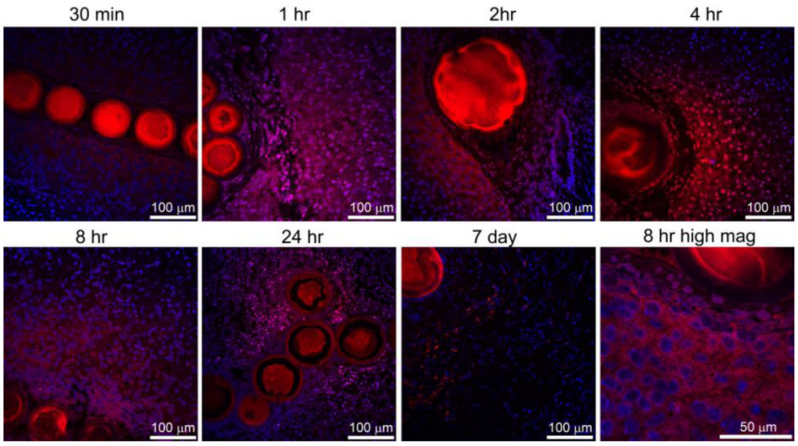

Figure 8.

Doxorubicin distribution surrounding radiopaque DEBs with confocal microscopy. Doxorubicin (red) and nuclei (blue) levels were adjusted to best appreciate the drug distribution. All images are identical magnification with 100 μm bar except for the higher magnification image at 8 hr included in lower right panel (bar = 50 μm). Both 70–150μm and 100–300 μm radiopaque DEBs are included in this figure. These DEBs were made radiopaque by the inclusion of Lipiodol inside the DEBs. From [77] with permission.

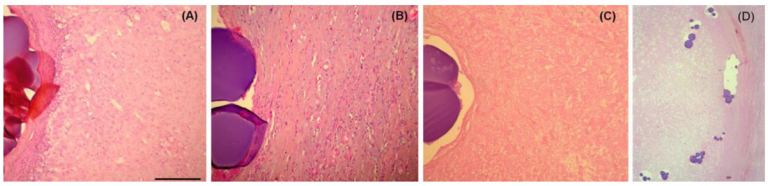

Figure 9.
DEB associated with (A) liver parenchyma, (B) inflammatory-fibrotic tissue or (C) necrotic tissue. Scale bar = 100μm for A, B and C. Modified from [75] with permission. (D) Low magnification overview of HCC tumor border (tumor on left and Liver on right) with extensive tumor necrosis. Courtesy of Drs. M. Wassef (Hospital Lariboisière) and S. Citron (Piedmont Hospital) [75].

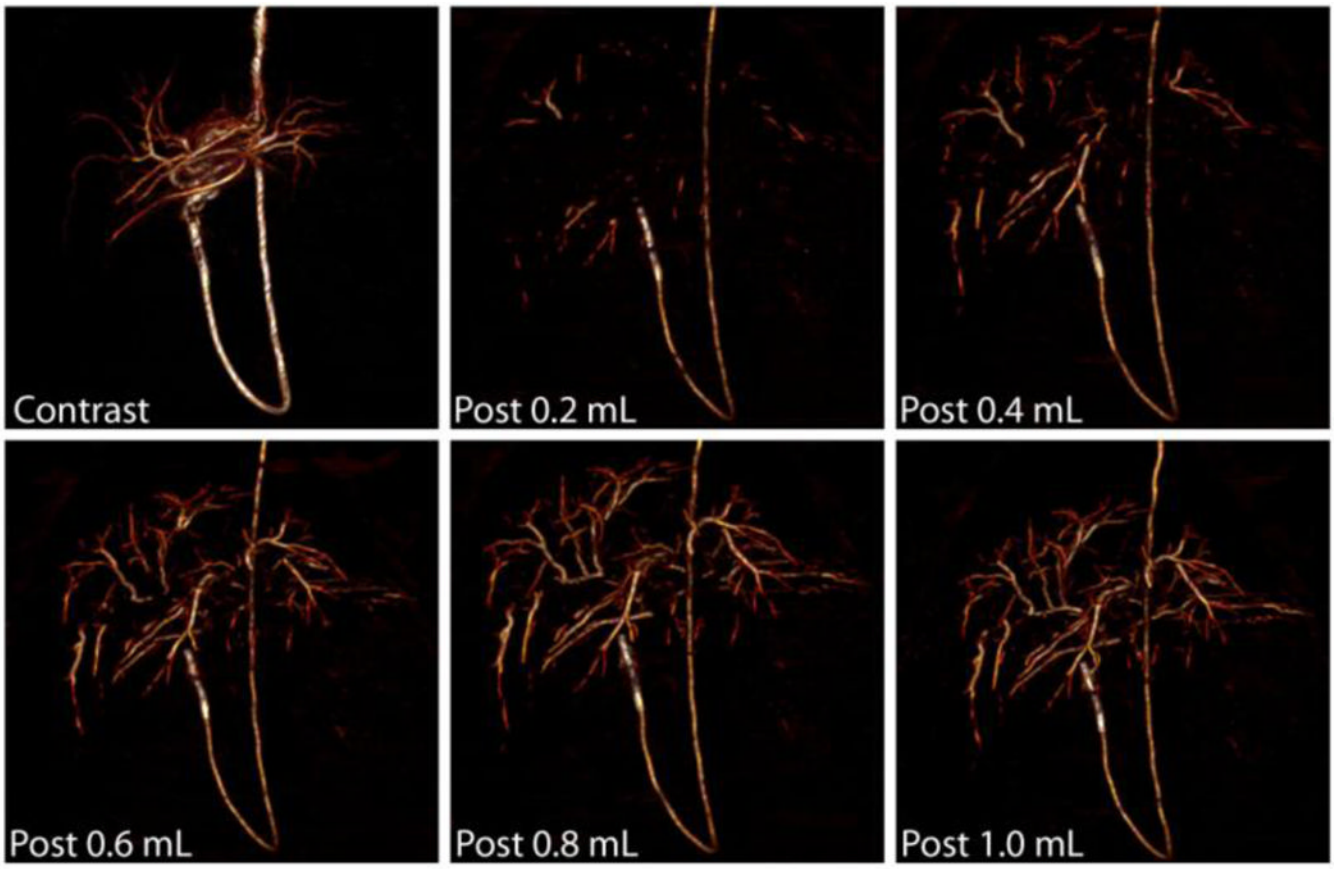

Figure 10.
Detection of radiopaque beads with CT during transcatheter embolization of swine liver. Representative three-dimensional surface-shaded display (SSD) images of swine liver reconstructed from data acquired with a clinical 16 detector row CT scanner during transcatheter embolization with radiopaque beads. The image labeled “Contrast” is from a pre-embolization transcatheter CT angiogram using dilute contrast. The other images were obtained following transcatheter embolization of 0.2 mL increments of radiopaque beads from the same catheter tip location within a lobar branch of the hepatic artery. From [85] with permission.

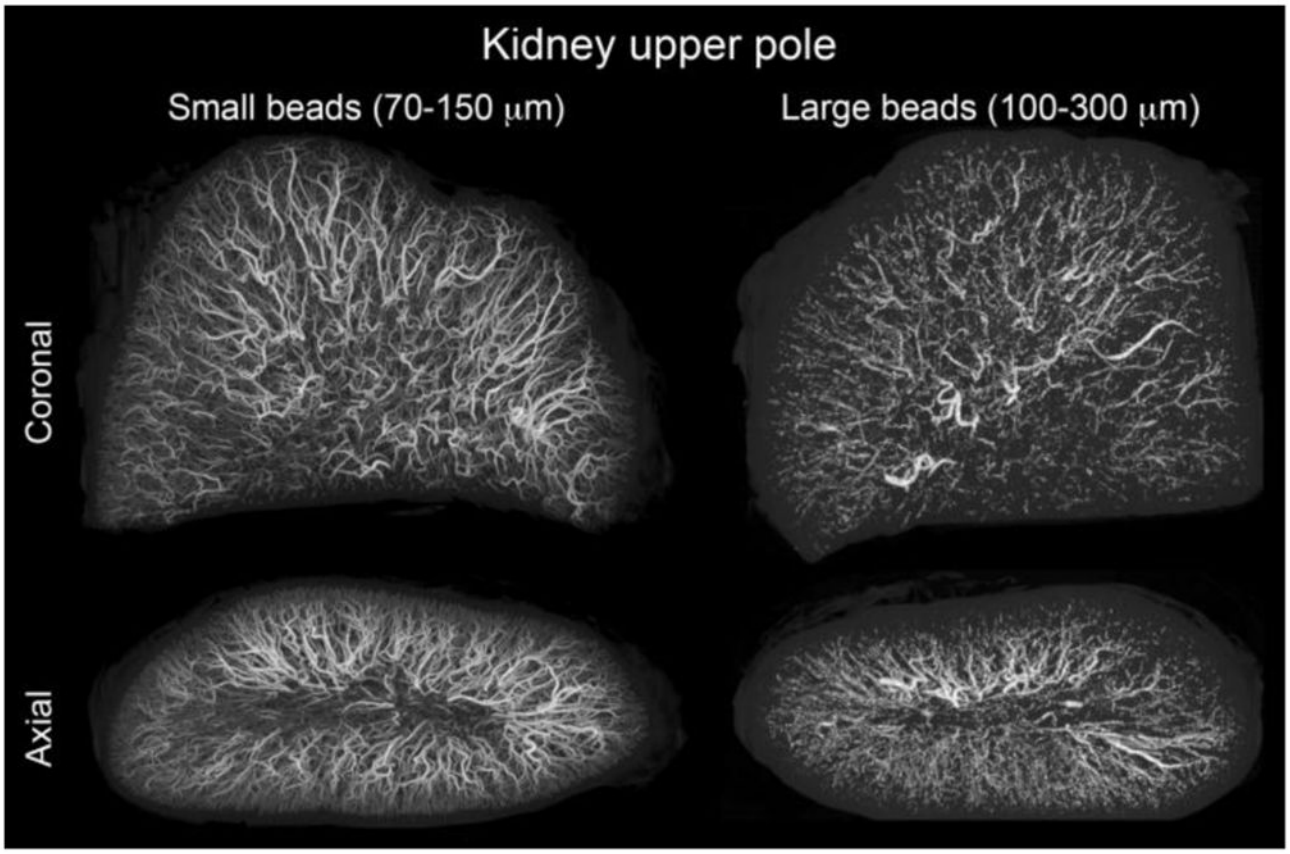

Figure 11.
microCT of swine kidney tissue embolized with radiopaque DEBs. Small size range (70–150 μm) and large size range (100–300 μm) DEBs are displayed with consistent size scaling. Small beads penetrate to more distal regions and yield a greater spatial density. These DEBs were made radiopaque by the inclusion of Lipiodol inside the DEBs. From [77] with permission.

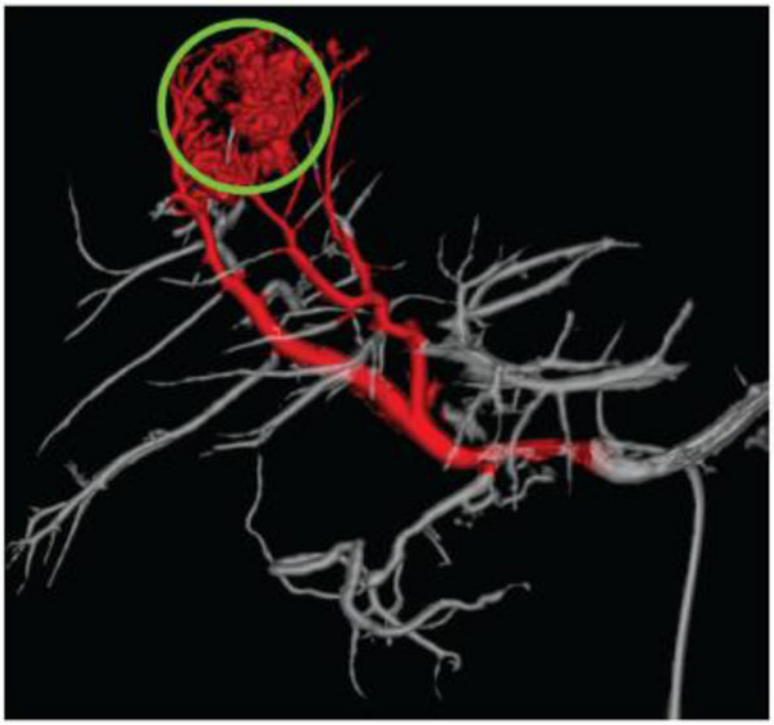

Figure 12.
Automatic identification of tumor feeding vessels (red) by a hepatic embolization treatment planning system. Tumor is indicated by a green circle. From [95] with permission.